Electronic Supplementary Material (ESI) for Soft Matter.

Electronic Supporting Information

Self-adaptive Hydrogels to Mineralization

Tooba Shoaib, Ariel Carmichael, R. E. Corman, Yun Shen, Helen Nguyen, Randy H. Ewoldt, Rosa M. Espinosa-Marzal

Optical Microscopy

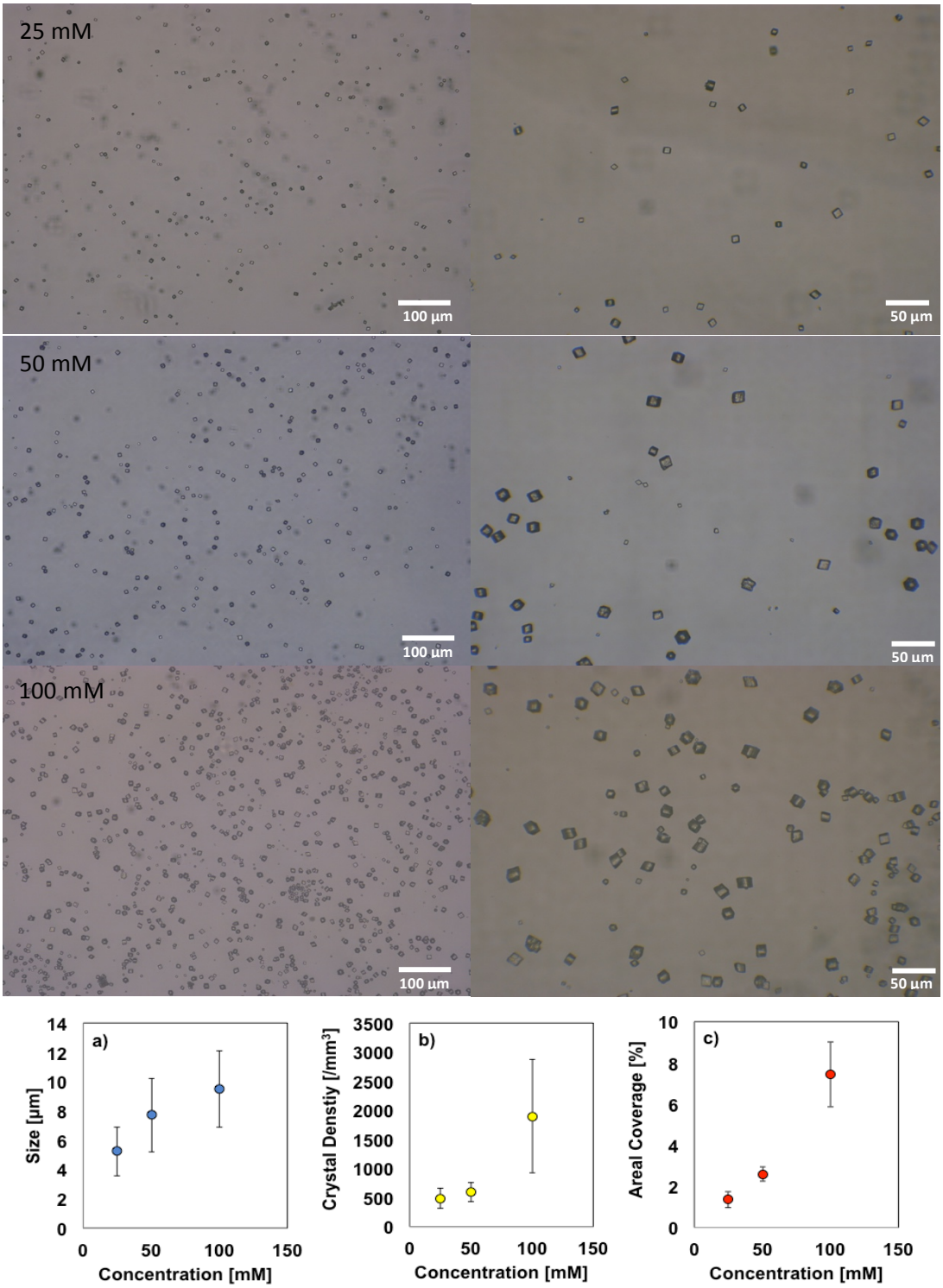

Figure S1: Top: Light microscopy images of $CaCO_3$-agarose hydrogels prepared with 25 mM, 50 mM and 100 mM $CaCO_3$ solution. Bottom: a) Size of calcite crystals, b) crystal density per unit volyme, and c) areal coverage at the focal plane as a function of concentration. Ion diffusion was possible through

all surfaces of the prepared samples, which led to crystallization across the depth of the hydrogels with two crystallization fronts.

Raman microspectroscopy

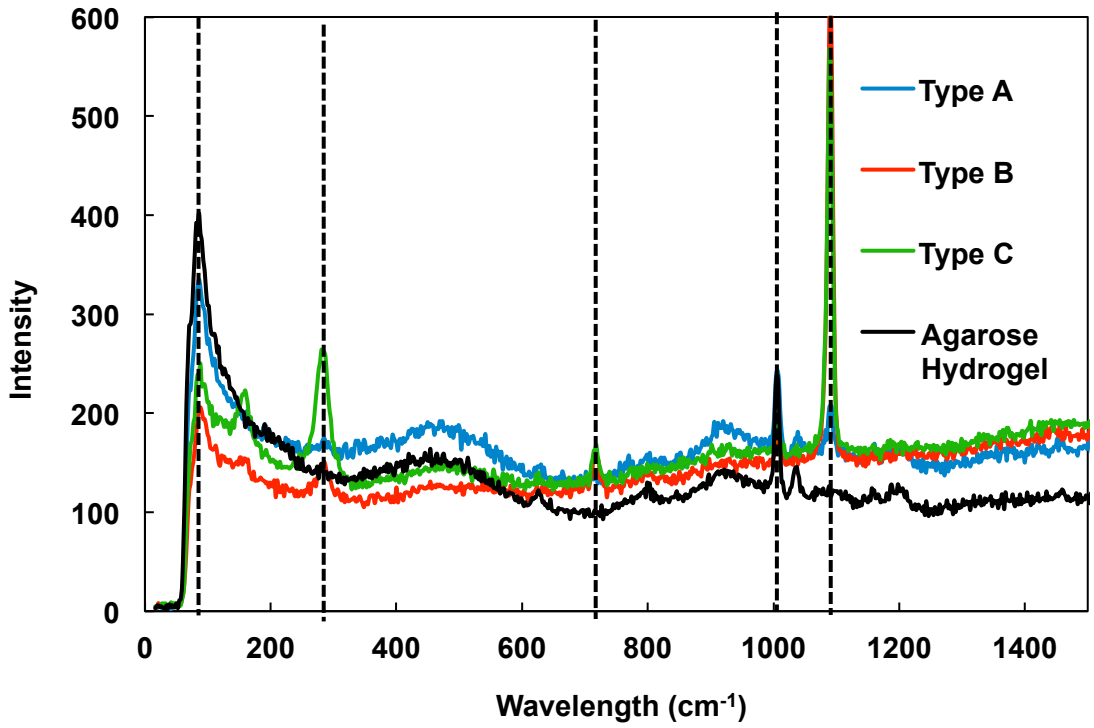

Figure S2: Raman spectroscopy of the representative spectra of reference and mineralized agarose gels. Three characteristic spectra for mineralized gels were detected in areas containing crystals, and they are labelled as Type A, B and C, depending on the calcite peaks that were detected: in Type A (1090 cm^{-1}), in Type B (282, 717, and 1090 cm^{-1}), and in Type C (157, 282, 717, and 1090 cm^{-1}). All spectra taken on mineralized gels contained at least one agarose peak (1005 cm^{-1}), while Type A showed an additional agarose peak (1606 cm^{-1}**,** not shown). This was attributed to the larger distance of crystals of type A from the surface, thereby leading to more prominent peaks for agarose.

Two of the calcite peaks observed in all measurements (~717 and 1090 cm^{-1}) differed slightly from reported values (713 and 1086 cm^{-1} [1]). The observed shift could result from a strong interaction between the mineral and the polymer. Although the latter peak observed at 1090 cm^{-1} is also characteristic of vaterite, the characteristic split peak of vaterite at 1090 cm^{-1} was not observed.[2] No other calcium carbonate polymorph was detected. Therefore calcite was the only detected crystal phase in the mineralized agarose gel.

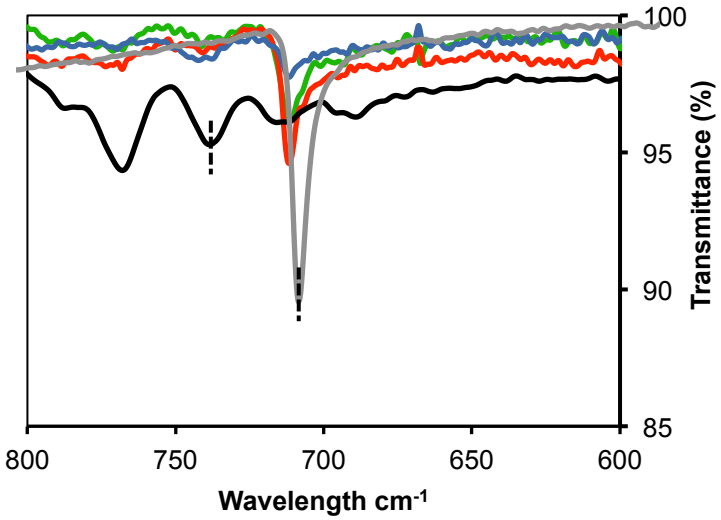

Figure S3: Fourier transform infrared spectroscopy (FTIR) spectra for $CaCO_3$-agarose gels. Color legend: 25mM (blue), 50 mM (green), and 100 mM (red). Reference: dry agarose in black, and calcite (grey). Peaks for $CaCl_2$ and Na_2CO_3 were not detected in the hydrogels. All mineralized gels show the calcite peak at 713 cm^{-1}.

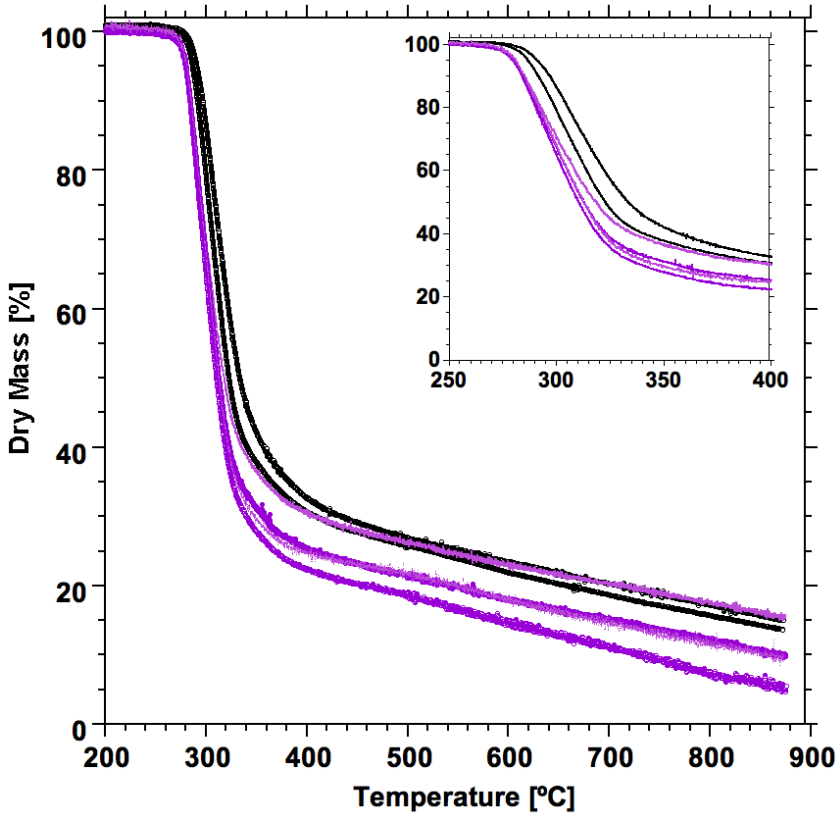

Figure S4: Thermal decomposition of reference agarose hydrogels (black) and of hydrogels prapared with DI water but stored in saturated calcium carbonate solution ($CaCO_3$-agarose 0.1 mM, in purple). The inset shows a magnification of the first decomposition. The first thermal decomposition is attributed to the degradation of the polymer regions with lower thermal stability, while the second

(slow) decomposition is attributed to the degradation of polymer regions with higher stability. The first onset temperature decreases with exposure to saturated calcium carbonate solution.
Since the first decomposition leads to a higher mass loss in the presence of calcium carbonate solution (77(1) vs. 72(2) wt%), a low calcium concentration increases the content in agarose strands with low stability. The average degradation rate (Δm/ΔT) during the second decomposition is similar for both systems, which means that the more thermally stable agarose strands have similar thermal stability.

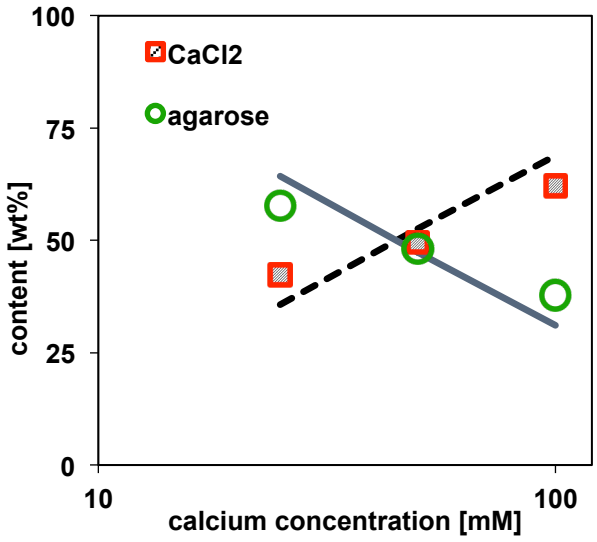

Figure S5: $CaCl_2$ and agarose contents in Ca-agarose hydrogels. The lines give the expected agarose and $CaCl_2$ content based on the stoichiometry of the bulk solution.

Drying in the TGA leads to precipitation of $CaCl_2$(s) in the Ca-agarose gels; $CaCl_2$ salt does not decompose within the investigated temperature range. The residual weight of the Ca-agarose gels, thus, includes salt and agarose. Since the amount of residual agarose is unknown, it was assumed to be the same in the reference hydrogel (11 wt%). The observed deviation from the stoichiometry of the bulk solution shown in Figure S5 implies that the ratio of $CaCl_2$ content per dry weight of agarose at 25mM is a bit larger than in the bulk solution, while this trend is inverted at the highest concentration of 100 mM.

Study of calcite decomposition by X-ray powder diffraction (XRD), Scanning Electron Microscopy (SEM) and FTIR

25mM, 50mM and 100mM $CaCO_3$ agarose hydrogels were prepared according to the usual protocol (each with 1ml of agarose solution). After mineralization, samples were rinsed and stored in saturated $CaCO_3$ solutions overnight at 6°C for further study. 40 hydrogels were prepared at each $CaCO_3$ concentration to obtain a sufficient amount of dry mass (~500 µg) for XRD, SEM and FTIR.
The hydrogel samples were placed in a high temperature and were heated up to the selected temperature (510°C, 600°C, and 900°C) at a rate of 10°C/min. The residue was used for studies by X-ray powder diffraction (XRD) with a Siemens-Bruker D5000 X-Ray Powder Diffraction System (TX, USA) and complementary IR spectroscopy. The XRD diffraction pattern was collected for 2-Theta angles between 20 and 60 degrees, with a 0.02 degree spacing and a scan speed of 2 degrees/minute. The SEM is a Hitachi S4700. Images were taken at a voltage of 10kV and a current of 10 µA. The samples were coated with Au/Pd for 30 seconds prior to imaging.

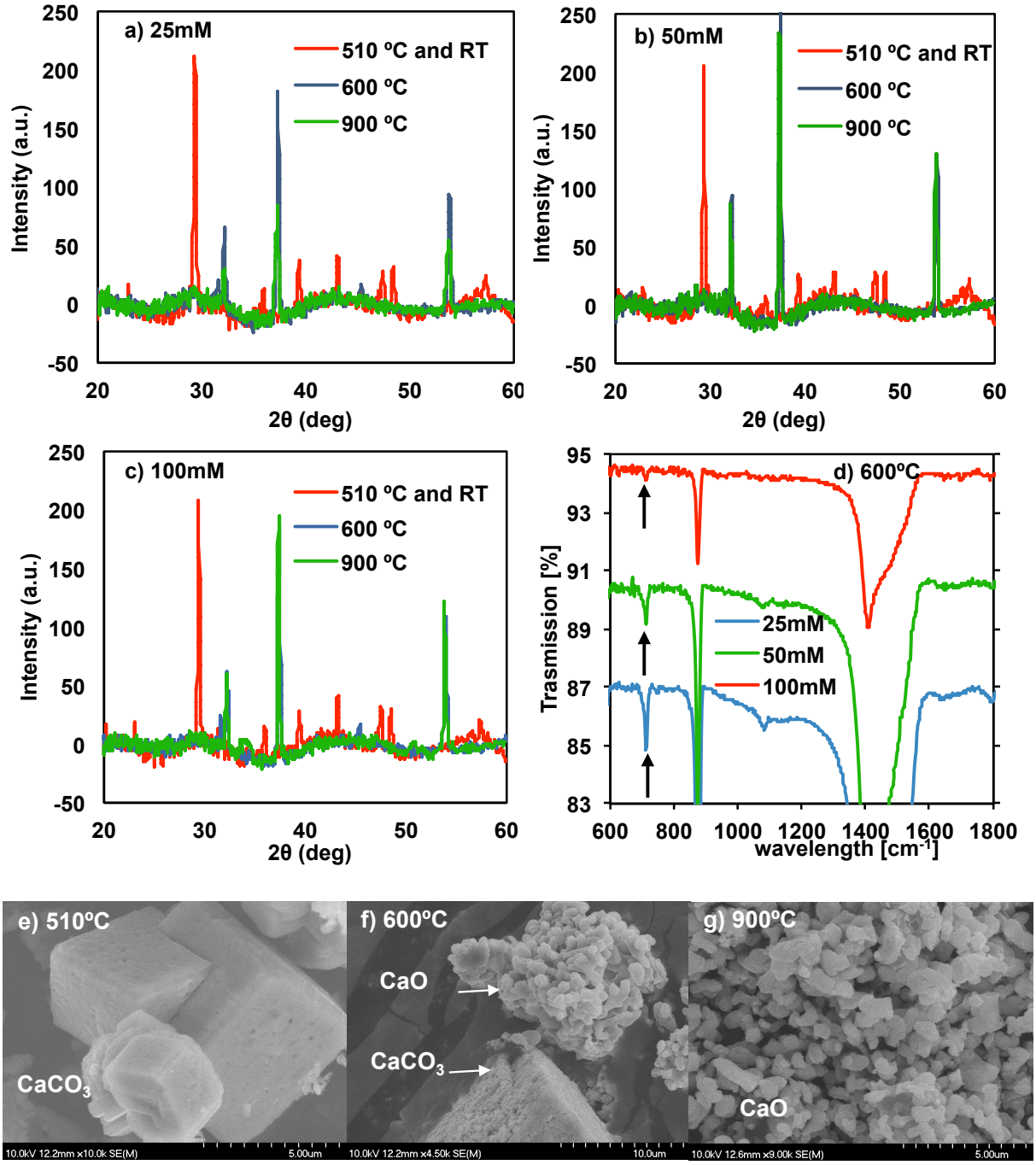

Figure S6: X-ray powder diffraction of a) 25mM, b) 50mM and c) 100 mM $CaCO_3$ hydrogels after thermal decomposition at 510ºC, 600ºC and 900ºC. The results at RT are not shown but they are identical to those at 510ºC. While the peaks characteristic of calcite can be seen at 510ºC, CaO can be identified already at 600ºC and at 900ºC at all concentrations; the diffractions detected for calcite (*) and for CaO (o) are the same at all concentrations. This demonstrates that the thermal decomposition of calcite (I) takes place between 510ºC and 600ºC. Several calcite crystals detected at 510ºC (and room temperature) have a roughened surface at the nanoscale. Previous work[3] has shown that calcite crystals etch in the hydrogel over time, while new crystals with nanometer size grow on the surface at the same time; this was also observed in our samples. Nanometer-size crystals display a lower calcination temperature due to their increased surface energy, as demonstrated, for instance, in ref. [4], which justifies the low temperature for the thermal decomposition of calcite (I).
SEM images confirm the presence of calcite and CaO at 600ºC (f). IR spectroscopy (d) clearly shows the presence of calcite at this temperature (see the peak at 712 cm^{-1}) as well, while calcite cannot be clearly detected at 600ºC by XRD. To detect a crystalline phase by XRD every possible crystalline orientation needs to be represented equally in the sample and be randomly arranged. We conclude that calcite (II) does not achieve true randomness in the prepared samples.

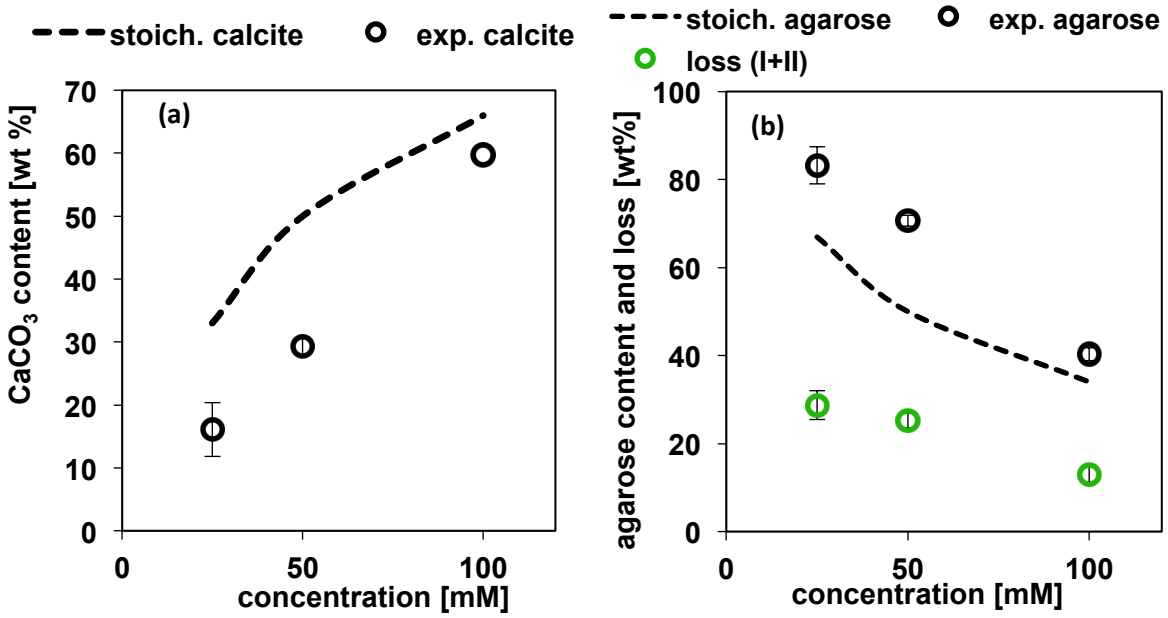

Figure S7: (a) Calcium carbonate content, and (b) agarose total content and loss during the two step-decomposition of the mineral (I and II) as a function of calcium concentration in mineralized $CaCO_3$-agarose hydrogels. The lines in a and b were obtained by considering the stoichiometry of the solution.

Since a distinction between the residual weight of agarose and CaO in CaCO3-agarose gels is not possible, the amount of calcium carbonate was estimated by an alternative method to that shown in Figure 3. It was assumed that the residual weight for agarose is the same as in the reference hydrogels (11 wt% of dry agarose). Based on this assumption, the weight % of calcite is smaller than given by the stoichiometry of the solution, and the content of agarose is significantly larger. The amount of agarose embedded into calcite can also be estimated from the weight loss during decomposition I+II. Such significant incorporation of agarose in calcite is consistent with previous works[5].

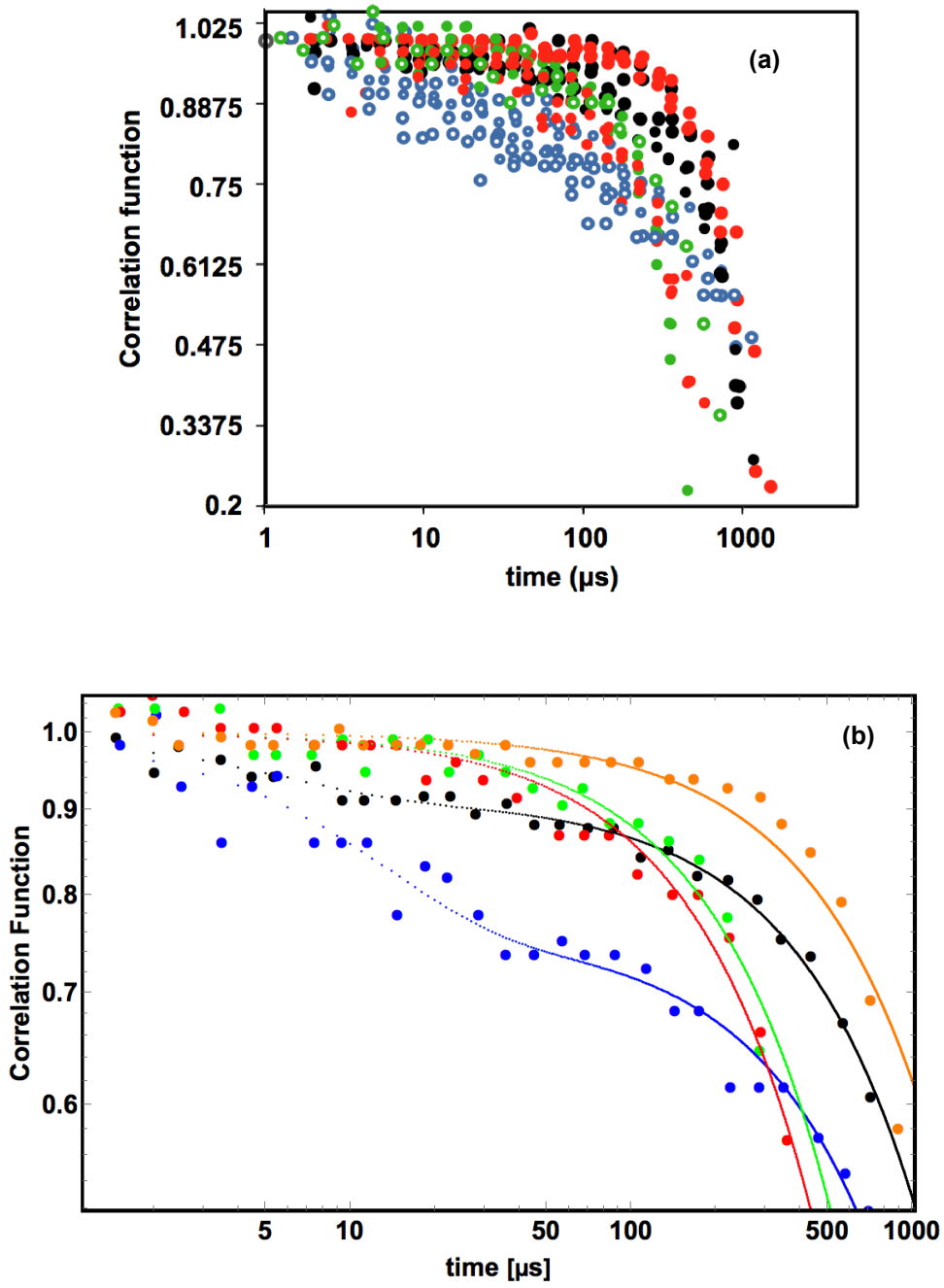

Figure S8: a) Correlation function as a function of time for reference hydrogels (black) and Ca-agarose gels at calcium concentrations of 25mM (blue), 50mM (green), and 100mM (red, orange), and b) representative fits to the correlation functions via a single exponential decay for 50 and 100mM Ca-agarose gels and a bi-exponential function for reference and 25mM Ca-agarose gels. The 100mM Ca-agarose gels exhibited two types of decay.

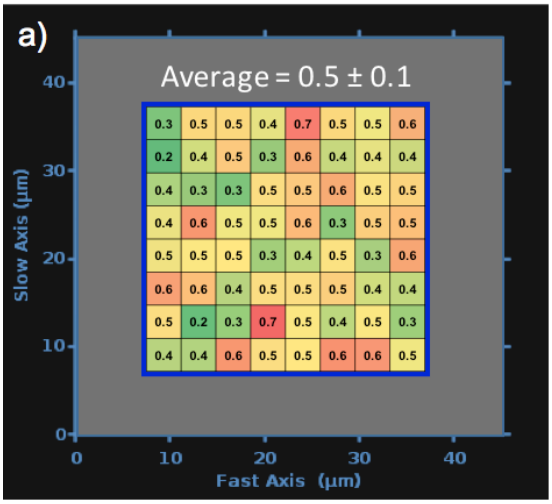
a)
Average = 0.5 ± 0.1
0.3 0.5 0.5 0.4 0.7 0.5 0.5 0.6
0.2 0.4 0.5 0.3 0.6 0.4 0.4 0.4
0.4 0.3 0.3 0.5 0.5 0.6 0.5 0.5
0.4 0.6 0.5 0.5 0.6 0.3 0.5 0.5
0.5 0.5 0.5 0.3 0.4 0.5 0.3 0.6
0.6 0.6 0.4 0.5 0.5 0.5 0.4 0.4
0.5 0.2 0.3 0.7 0.5 0.4 0.5 0.3
0.4 0.4 0.6 0.5 0.5 0.6 0.6 0.5
Slow Axis (µm)
Fast Axis (µm)
0
10
20
30
40

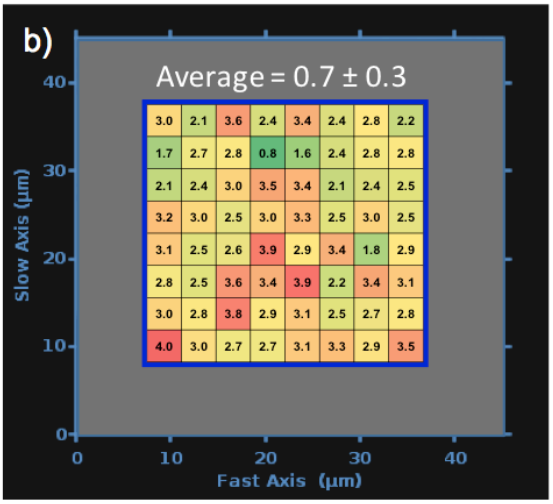
b)
Average = 0.7 ± 0.3
3.0 2.1 3.6 2.4 3.4 2.4 2.8 2.2
1.7 2.7 2.8 0.8 1.6 2.4 2.8 2.8
2.1 2.4 3.0 3.5 3.4 2.1 2.4 2.5
3.2 3.0 2.5 3.0 3.3 2.5 3.0 2.5
3.1 2.5 2.6 3.9 2.9 3.4 1.8 2.9
2.8 2.5 3.6 3.4 3.9 2.2 3.4 3.1
3.0 2.8 3.8 2.9 3.1 2.5 2.7 2.8
4.0 3.0 2.7 2.7 3.1 3.3 2.9 3.5
Slow Axis (µm)
Fast Axis (µm)
0
10
20
30
40

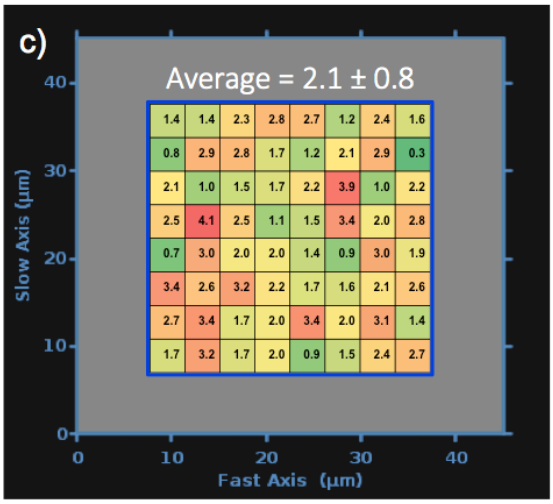
c)
Average = 2.1 ± 0.8
1.4 1.4 2.3 2.8 2.7 1.2 2.4 1.6
0.8 2.9 2.8 1.7 1.2 2.1 2.9 0.3
2.1 1.0 1.5 1.7 2.2 3.9 1.0 2.2
2.5 4.1 2.5 1.1 1.5 3.4 2.0 2.8
0.7 3.0 2.0 2.0 1.4 0.9 3.0 1.9
3.4 2.6 3.2 2.2 1.7 1.6 2.1 2.6
2.7 3.4 1.7 2.0 3.4 2.0 3.1 1.4
1.7 3.2 1.7 2.0 0.9 1.5 2.4 2.7
Slow Axis (µm)
Fast Axis (µm)
0
10
20
30
40

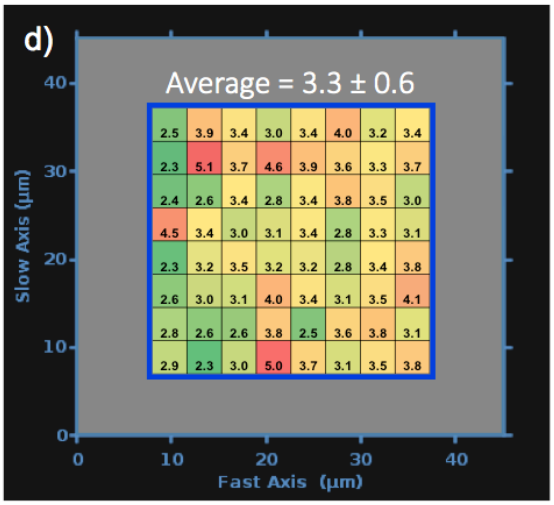
d)
Average = 3.3 ± 0.6
2.5 3.9 3.4 3.0 3.4 4.0 3.2 3.4
2.3 5.1 3.7 4.6 3.9 3.6 3.3 3.7
2.4 2.6 3.4 2.8 3.4 3.8 3.5 3.0
4.5 3.4 3.0 3.1 3.4 2.8 3.3 3.1
2.3 3.2 3.5 3.2 3.2 2.8 3.4 3.8
2.6 3.0 3.1 4.0 3.4 3.1 3.5 4.1
2.8 2.6 2.6 3.8 2.5 3.6 3.8 3.1
2.9 2.3 3.0 5.0 3.7 3.1 3.5 3.8
Slow Axis (µm)
Fast Axis (µm)
0
10
20
30
40

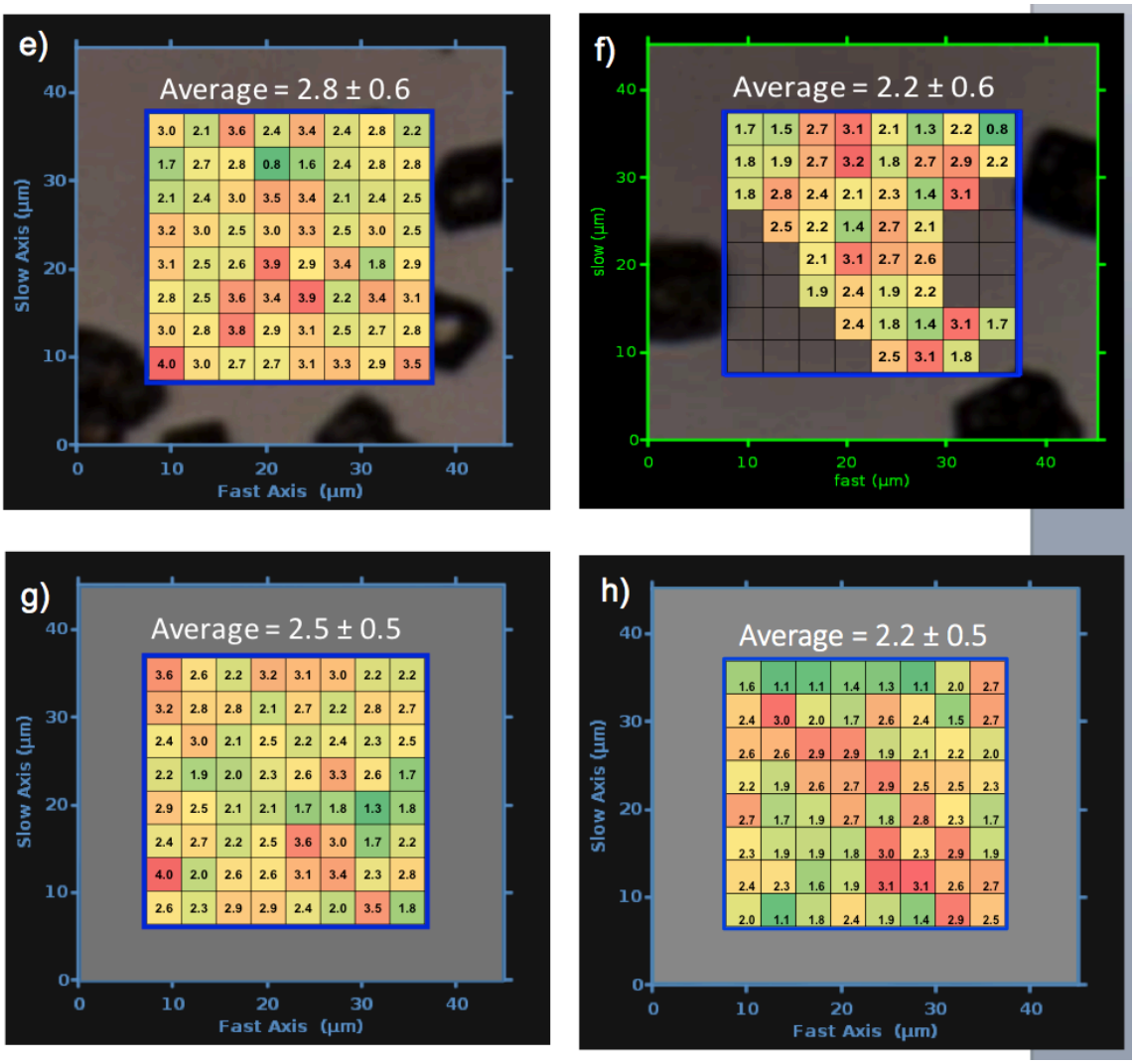

Figure S9: Elastic modulus 2D-maps for (a) agarose reference gel, (b) $CaCO_3$-agarose gel in 0.1mM $CaCO_3$ solution, (c) Ca-agarose gel in 25mM $CaCl_2$, and (d) in 50 mM $CaCl_2$, $CaCO_3$-agarose gels in (e) 25 mM $CaCO_3$ and (f) in 50 mM $CaCO_3$, close to crystals (black in images), and (g) $CaCO_3$-agarose gels in (g) 25 mM $CaCO_3$ and (h) in 50 mM $CaCO_3$, far away from crystals.

All gels were prepared under the same conditions (same agarose concentration in the bulk solution and temperature). Since evaporation is possible during gelation, the water content can slightly vary across samples, which can explain part of the variability of the elastic modulus across experiments. For example, a decrease of 0.2% of water leads to a notable increase in agarose concentration (from 0.5 weight % to 0.7 weight %) and to a three-fold larger stiffness[6].

References

1. S. N. White, *Chemical Geology*, 2009, **259**, 240-252.
2. G. Behrens, L. T. Kuhn, R. Ubic and A. H. Heuer, *Spectroscopy letters*, 1995, **28**, 983-995.
3. L. A. Estroff, L. Addadi, S. Weiner and A. D. Hamilton, *Org Biomol Chem*, 2004, **2**, 137-141.
4. R. Babou-Kammoe, S. Hamoudi, F. Larachi and K. Belkacemi, *Can J Chem Eng*, 2012, **90**, 26-33.

5. H. Li and L. A. Estroff, *Advanced Materials*, 2009, **21**, 470-473.
6. V. Normand, D. L. Lootens, E. Amici, K. P. Plucknett and P. Aymard, *Biomacromolecules*, 2000, **1**, 730-738.